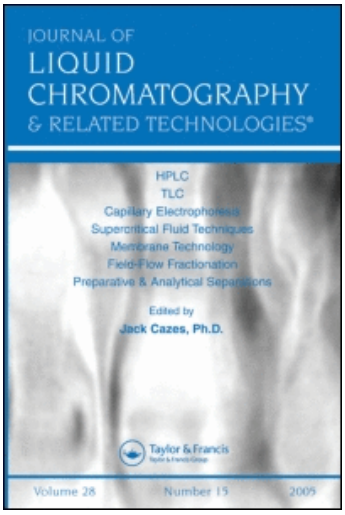

Journal of Liquid Chromatography & Related Technologies
Publication details, including instructions for authors and subscription information:
http://www.informaworld.com/smpp/title~content=t713597273

MICRO-CHANNEL THERMAL FIELD-FLOW FRACTIONATION: NEW CHALLENGE IN ANALYSIS OF MACROMOLECULES AND PARTICLES

Josef Janca[a]
[a] Ple Sciences et Technologie, Université de La Rochelle, 17042 La Rochelle, France

Online publication date: 23 April 2002

To cite this Article Janca, Josef(2002) 'MICRO-CHANNEL THERMAL FIELD-FLOW FRACTIONATION: NEW CHALLENGE IN ANALYSIS OF MACROMOLECULES AND PARTICLES', Journal of Liquid Chromatography & Related Technologies, 25: 5, 683 — 704
To link to this Article: DOI: 10.1081/JLC-120003028
URL: http://dx.doi.org/10.1081/JLC-120003028

J. LIQ. CHROM. & REL. TECHNOL., 25(5), 683–704 (2002)

MICRO-CHANNEL THERMAL FIELD-FLOW FRACTIONATION: NEW CHALLENGE IN ANALYSIS OF MACROMOLECULES AND PARTICLES

Josef Janca

Université de La Rochelle, Pôle Sciences et Technologie,
Avenue Michel Crepeau, 17042 La Rochelle,
Cedex 01, France
E-mail: jjanca@univ-lr.fr

ABSTRACT

The operational variables in Thermal Field-Flow Fractionation (TFFF) and the parameters of the separation channel were studied theoretically and experimentally in order to optimize the design of the channel. As a result, a new micro-channel, which allows high-performance separations under carefully chosen experimental conditions, was conceived and built up. This new micro-(μ)-TFFF becomes highly competitive compared with microcolumn chromatography of macromolecules in the range of molar masses up to roughly one million g/mole. However, the versatility of μ-TFFF is superior over the column chromatographic methods due to its capacity to fractionate the

macromolecules of ultra-high molar masses, and even the colloidal particles. Although this work concerns, exclusively, the μ-TFFF, the miniaturization of the separation channel can generally be applied to other FFF methods as well.

INTRODUCTION

Thermal Field-Flow Fractionation, invented and applied experimentally for the separation of polystyrenes in 1967 (1), is the oldest of all FFF methods. Its universal applicability for the fractionation of various polymers was demonstrated in 1978.(2) Many various applications of TFFF for the analysis of polymers and colloidal particles were published and reviewed.(3,4) The utilized TFFF channels, available commercially (5), as well as homemade ones (6), have almost the same size and design as those constructed at the very beginning.(1) The usual dimensions are roughly $50 \times 2 \times 0.01$ cm. The theoretical and practical aspects of reducing the dimensions of FFF channels were treated by Giddings (7) in 1993; however, the only study whose goal was to increase the performance of the TFFF due to the reduced thickness of the channel was already published in 1978.(8) Nevertheless, the other dimensions of the channel were kept practically unchanged.

The aim of this study is to show both theoretically and experimentally, that a substantial miniaturization of the TFFF channel results not only in high-performance separations, but also in dramatically reduced carrier liquid and energy consumption. The minimized carrier liquid flow rate opens the possibility of on-line coupling of the μ-TFFF with mass spectroscopy and, thus, allows a more detailed analysis of the fractionated species, reserved until now exclusively to microcolumn liquid chromatography. A crucial lowering of energy consumption represents, undoubtedly, an economic interest but, what is more important, it extends substantially the range of the temperature gradients that can be reached at lower heat fluxes and it allows working at much lower temperatures of the cold wall. Such experimental conditions cannot be employed with TFFF channels of classical size due to the extreme difficulty to evacuate an enormous heat flux between the hot and cold walls by the current refrigerating thermostats. Although most applied cooling by tap water is efficient, it does not allow control of the cold wall temperature. The variation of the experimental conditions is more versatile with the μ-TFFF channel, the separations are easier to be carried out, and the mass of the fractionated samples can be reduced to a few nanograms.

THEORETICAL ANALYSIS

Efficiency

The efficiency in FFF is characterized by the height equivalent to a theoretical plate (9).

$$H = \frac{2D}{R\langle v\rangle} + \frac{\chi^{w^2}\langle v\rangle}{D} + \sum H_i \tag{1}$$

where D is the diffusion coefficient of the fractionated species, R is the retention ratio, $\langle v\rangle$ is the average linear velocity of the carrier liquid inside the channel, w is the thickness of the channel, the sum of H_i represents the extra-channel contributions to the plate height, and χ is a dimensionless parameter. The first term in the Equation (1) describes the longitudinal diffusion and the second one corresponds to the nonequilibrium (mass transfer) processes. It holds for χ (10):

$$\chi = \frac{24\lambda^3}{1 + \exp(-1/\lambda) - 2\lambda(1 - \exp(-1/\lambda))} \times B \tag{2}$$

where B is:

$$B = (28\lambda^2 + 1)\left(1 - \exp\left(\frac{-1}{\lambda}\right)\right) - 10\lambda\left(\exp\left(\frac{-1}{\lambda}\right) + 1\right) - \frac{1}{3\lambda^2} - \frac{2}{\lambda} + 4 - \frac{1/\lambda}{1 - \exp(1/\lambda)}\left[4\lambda\left(1 + \frac{1/\lambda}{1 - \exp(1/\lambda)}\right) - \frac{1}{3\lambda} - 6\right] \tag{3}$$

The dimensionless parameter $\Lambda = l/w$ is the ratio of the distance l of the center of gravity of the concentration distribution across the channel of the retained species from the accumulation wall to the channel thickness w. The Λ is related to the retention ratio R by the well-known relationship (9):

$$R = 6\lambda\left[\coth\left(\frac{1}{2\lambda}\right) - 2\lambda\right] \tag{4}$$

An optimal average linear velocity of the carrier liquid can be calculated from Equation (1) as:

$$\langle v\rangle_{opt} = \frac{\partial H}{\partial\langle v\rangle} = 0 \tag{5}$$

The result is:

$$\langle v\rangle_{opt} = \frac{D}{w}\sqrt{\frac{2}{\chi^R}} \tag{6}$$

Alternatively, the optimal average linear velocity of the retained species can be calculated from:

$$\langle v\rangle_{R,opt} = R\langle v\rangle_{opt} = \frac{D}{w}\sqrt{\frac{2R}{\chi}} \tag{7}$$

The optimal average linear velocity, calculated for the retained polymers of molar masses from 10^4 to 10^6 g/mole (for which the diffusion coefficients in common solvents lie roughly (11) within $D = 10^{-6}$ to 10^{-8} cm^2/sec) by using the input values of $w = 0.005$ cm and $\Lambda = 0.01$ to 0.4, reaches the maximal value of 0.014 cm/sec for highly retained ($\Lambda = 0.01$), low molar mass species ($D = 10^{-6}$ cm^2/sec), but it decreases very rapidly with increasing Λ and w values. Consequently, the first term in Equation (1) describing the contribution of the longitudinal diffusion can be neglected in all practical cases (due to low optimal velocities). This result has intuitively been anticipated (6).

As mentioned in the Introduction, the only study of optimization of the TFFF channel concerned its reduced thickness w. A positive impact of such a modification is due to the second power of the w in the second term (mass-transfer contribution) in the Equation (1). Unfortunately, the reduced thickness w of the channel leads to the proportional increase of the heat flux across the channel if the temperature drop between the channel walls and, consequently, the retentions, have to be kept unchanged. As a result, the electrical power needed to heat the hot wall can reach kilowatts and, of course, the same energy flux has to be evacuated from the cold wall.

A more elegant way to reach higher performance of the TFFF channel consists in increasing the temperature drop by keeping the thickness of the channel unchanged. The consequence is as follows. The retention parameter Λ is related to the temperature drop ΔT across the channel of the thickness w by:

$$\lambda = \frac{T}{\alpha_T \Delta T} \tag{8}$$

where T is the temperature and α_T is the thermal diffusion factor. Thus, it holds for the variation of the retention parameter Λ due to the variation of the temperature gradient:

$$\lambda_2 = \lambda_1 \frac{\Delta T_1}{\Delta T_2} \tag{9}$$

The relative variation of the efficiency H_2/H_1 can be calculated from the mass transfer term in Equation (1) by using the Equations (2), (3), and (8). The result of this calculation is shown in Figure 1. The accurate dependence:

$$\frac{H_2}{H_1} = f\left(\frac{\chi_2}{\chi_1}\right) = f'\left(\frac{\lambda_2}{\lambda_1}\right) = f''\left(\frac{\Delta T_1}{\Delta T_2}\right) \tag{10}$$

represented in Figure 1 (black curve) can be approximated by:

$$\frac{H_2}{H_1} = \left(\frac{\Delta T_1}{\Delta T_2}\right)^{2.8} \tag{11}$$

(gray curve) which is close to that obtained by using a limit relationship (9).

$$\lim_{\lambda \to 0} \chi = 24\lambda^3 \tag{12}$$

As a result, an increase of the temperature drop ΔT between the channel walls has a more pronounced effect on the efficiency compared with a decrease of the channel thickness w (see Equation (1)), accompanied by the same energy flux increase.

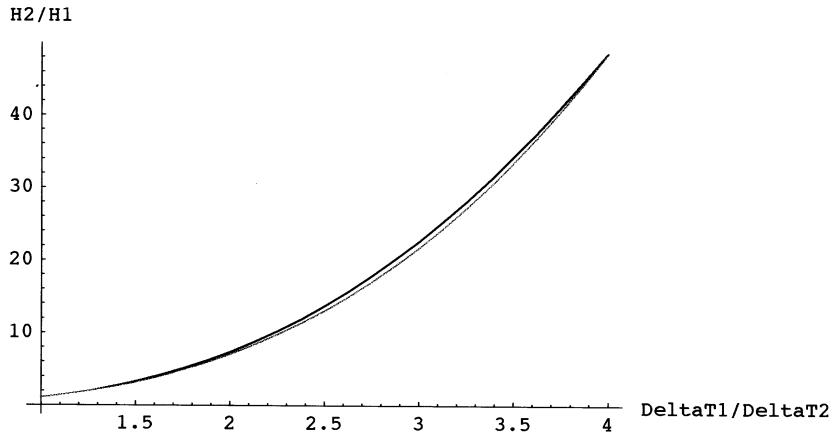

Figure 1. Relative variation of the efficiency H_2/H_1 with relative temperature drop $\Delta T_1/\Delta T_2$. Black curve was calculated from the accurate Equation (10); gray curve corresponds to the approximate Equation (11).

Resolution

The relationship defining the resolution R_s in FFF was derived by Martin and Jaulmes.(12) It can be modified conveniently to give:

$$R_s = \frac{\sqrt{L}|1/R_1 - 1/R_2|}{2(\sqrt{H_1}/R_1 + \sqrt{H_2}/R_2)} \tag{13}$$

where $R_{1,2}$ and $H_{1,2}$ are the retention ratio and the plate height, respectively, for two retained species 1 and 2, L is the length of the channel. By combining the Equation (13) with the second term of the Equation (1), we obtain:

$$R_s = \left(\frac{\sqrt{L}}{2w\sqrt{\langle v\rangle}}\right)\left[\frac{|1/R_1 - 1/R_2|}{\sqrt{\chi_1/D_1}/R_1 + \sqrt{\chi_2/D_2}/R_2}\right] \tag{14}$$

The R, χ, and D depend on the molecular characteristics of the retained species for given experimental conditions. On the other hand, the operational variables and channel parameters L, w, and $\langle v\rangle$ are interrelated, which means that a shortening of the channel accompanied by a corresponding decrease of the average linear velocity of the carrier liquid keeps the resolution unchanged. Consequently, the energy flux can be reduced proportionally to the shortening of the channel length. The other gain can be obtained by a proportional decrease of the thickness w of the channel and of its breadth b (the aspect ratio w/b does not change), which leads to an increase of the resolution by keeping the energy flux unchanged.

A review of the published papers on TFFF shows that the average linear velocities of the carrier liquid applied in the experiments are largely above the optimal ones. This is due to very low theoretical values of the optimal average linear velocities. As a result, a decrease of the currently used flow rates, necessary to compensate the shortening of the channel, should not represent a principal problem for practical TFFF experiments.

Extra-Channel Zone Broadening

The extra-channel contribution to the zone broadening (the third term in the Equation (1)) is due to the injection system, detector, and connecting capillaries. The introduction of a sample into the channel by a syringe through a septum, used in some old FFF apparatuses, eliminates the connecting capillary. Nevertheless, the use of an injection valve (2) has many practical advantages and an additional zone broadening in the capillary connecting the valve with the channel has no importance because the zone of the injected sample is, in fact, sharpened at the entry of the channel due to the retention. Moreover, if necessary,

this concentrating effect can be amplified by a temporary increase of the temperature drop during the injection. On the other hand, the detection system, including the capillary connecting the separation channel with an extra-channel measuring cell, should not increase the width of the zone of the retained species over the uncertainty of its measurement. This problem has already been studied in Size Exclusion Chromatography (13) and its solution can be transposed to the FFF. According to the rule of additivity of variances, the total variance σ_T^2 of the retained zone is the sum of the contributions to the zone broadening due to the channel, σ_C, and the detector, σ_D, (by supposing that the contribution due to the injection system, σ_I, can be neglected as mentioned above):

$$\sigma_T^2 = \sigma_C^2 + \sigma_D^2 \tag{15}$$

Consequently, if an acceptable uncertainty of the determination of the zone width σ_T measurement lies within 1 to 2%, the σ_D due to the detection system can be as high as 14 to 20% of the σ_C.

The calculation of the theoretical value of σ_C can be performed by combining the Equations (1) and (6) with the definition of the H based on experimentally available data:

$$H = L\left(\frac{\sigma_V}{V_R}\right)^2 \tag{16}$$

where V_R is the retention volume of a retained monodisperse species and σ_V alias σ_C is the standard deviation of the zone width expressed in coherent volume units. Thus, it holds for an optimal $\sigma_{V,\,opt}$ value:

$$\sigma_{V,opt}^2 = \left(\frac{2D}{R\langle v\rangle_{opt}} + \frac{\chi^{w^2}\langle v\rangle_{opt}}{D}\right)\frac{V_0^2}{R^2 L} \tag{17}$$

where $V_0 \approx \omega \Lambda \beta$ is the void volume of the channel and $R = V_0/V_R$. A rearrangement gives the result valid for the optimal average linear velocity of the carrier liquid:

$$\sigma_{V,opt} = \left[Lb^2 w^3 \sqrt{\frac{8\chi}{R^5}}\right]^{0.5} \tag{18}$$

In the case of an average linear velocity higher than the optimal one, the longitudinal diffusion term in Equation (1) can be neglected and the result is:

$$\sigma_V = \left[Lb^2 w^4 \frac{\chi\langle v\rangle}{DR^2}\right]^{0.5} \tag{19}$$

The results of the calculations using the Equation (19) and the dimensions $L = 10$ cm, $b = 0.5$ cm, $w = 0.005$ cm, and $D = 10^{-7}$ cm^2/sec are demonstrated in

Figure 2 as the dependence of σ_V on Λ for the optimal average linear velocity (gray curve) and for an arbitrarily chosen $\langle v \rangle = 0.1$ cm/sec (black curve), respectively. The standard deviation of the zone width of a retained monodisperse species σ_V varies (for a practical range of Λ values) between 0.5 to 2 μL in the first case and between 4 to 8 μL in the second one. If the channel dimensions are $L = 10$ cm, $b = 1$ cm, and $w = 0.01$ cm, the σ_V varies from 3 to 12 μL and from 30 to 60 μL, respectively. The contribution to the zone broadening caused by a detection system should satisfy the above mentioned condition resulting from the Equation (15):

$$\sigma_D \approx (0.14 \text{ to } 0.20) \times \sigma_v \tag{20}$$

As a result, the detection system has to be constructed correspondingly.

The theoretical analysis clearly indicates that the miniaturization of the TFFF channel can improve the performance of this technique. A similar result has recently been found for Electrical FFF.(14) The aim of our experimental work was to check the above theoretical conclusions concerning the design of a new microchannel for high performance TFFF and to demonstrate its applicability for the separation of polymers and particles.

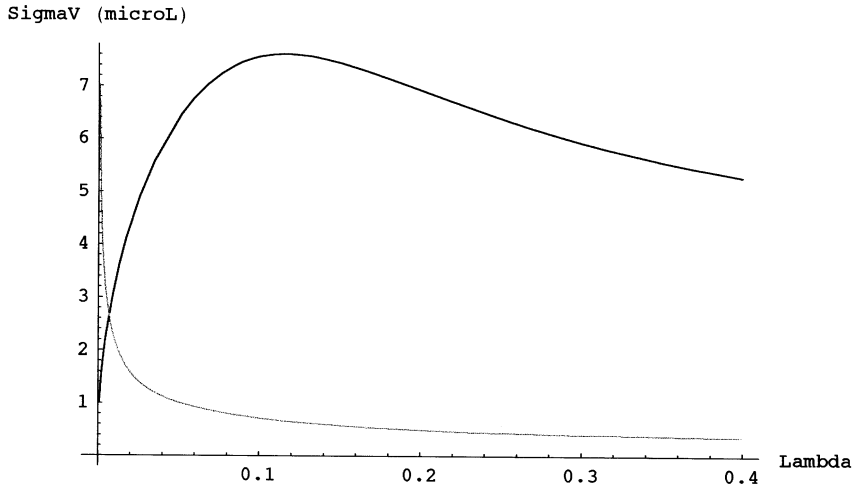

Figure 2. Dependence of the standard deviation of the zone of a retained monodisperse species, σ_V, as a function of the retention parameter Λ. Gray curve was calculated for an optimal linear velocity of the carrier liquid from the Equation (18) and for $L = 10$ cm, $w = 0.005$ cm, $b = 0.5$ cm, and $D = 10^{-7}$ cm^2/sec; black curve corresponds to the linear velocity $\langle v \rangle = 0.1$ cm/sec under the same conditions.

EXPERIMENTAL

μ-TFFF Equipment

The apparatus for the μ-TFFF consisted of an Intelligent Pump Model PU-980 (Jasco, Japan) able to work within the flow rate range from 1 μL/min to 10 mL/min, the injection valve Model 7410 (Rheodyne, USA) equipped with a 1 or 5 μL loop, the UV-VIS variable wavelength Intelligent detector Model UV-975 (Jasco, Japan) with the 1 μL measuring cell, and the recorder-integrator Model HP 3395 (Hewlett-Packard, USA).

The versatile fractionation μ-channel was constructed in such a manner that the thickness w and the void volume V_0 could easily be changed from $V_0 = 10.9$ to 225 μL for $w = 23$, 50, 100, and 250 μm. The form of highly polished contact surface of the hot and cold walls was designed and machined to minimize the area of high density heat flux and to assure a perfect seal of the channel. The volume of the capillaries connecting the entry of the μ-channel with the injection valve and the end of the channel with the detector was minimized to 3 μL.

The interchangeable heating cartridge of 200 W enabled reaching the temperature difference across the channel of approximately $\Delta T = 80$ K. The cold wall was cooled by a circulating liquid by using a compact low temperature thermostat (working range: -30°C to 100°C) Model RML 6 B (Lauda, Germany) of maximal refrigerating power of 350 W and providing a flow rate of 8 l/min. If necessary, the electrical heating cartridge could easily be changed to reach a maximal power of 600 W, which should enable working at as high a temperature difference as $\Delta T = 200$ K.

The electric power was regulated by an electronic variator and the temperatures of the cold and hot walls were measured by a Digital thermometer (Hanna Instruments, Portugal) equipped with two thermocouples. For security reasons, the channel was equipped with a maximal temperature controller, which automatically turns off the electric power if the temperature reaches the predetermined value.

Carrier Liquids and Polymer Samples

The tetrahydrofuran (THF) for HPLC (Carlo Erba, Italy) was used as a carrier liquid for the μ-TFFF of polystyrene standards. Polystyrene (PS) standards of various well defined molar masses (Polysciences, Inc., USA, Knauer, Germany, and Waters Associates, USA) were used as model samples of soluble polymers. Molar masses of all studied samples are given in Table 1.

Table 1. Molar Masses of Polystyrene Standards

Polystyrene Standard	$M_w \times 10^{-3}$ (g/mole)	$M_n \times 10^{-3}$ (g/mole)	Polydispersity (M_w/M_n)
PS 51 000	51	49	1.04
PS 11 1000	111		
PS 11 5000	115		<1.04
PS 23 3000	233		
PS 41 1000	411	392	1.05
PS 1 030 000	1,030		<1.06
PS 2 145 000	2,145	1780	1.21
PS 3 000 000	3,000		<1.2
PS 10 000 000	10,000		

RESULTS AND DISCUSSION

Zone Broadening Due to the Injector and Detector

The contribution to the zone broadening due to the injection and detection systems was studied experimentally by using the injection valve connected directly to the detector cell, with a capillary of the inner diameter and length equal to the diameter and the total length of the capillaries, which connect the injector and the detector with the channel in normal TFFF configuration. The broadening due to the detection system, σ_D, was determined from the standard deviation of the zone of a marker, σ_M, obtained by the injection of 1 μL of a diluted solution of toluene in THF:

$$\sigma_D = \sigma_M/\sqrt{2} \quad \text{by assuming that } \sigma_M^2 = \sigma_D^2 + \sigma_I^2 \text{ and } \sigma_D^2 = \sigma_I^2 \tag{21}$$

It has been found, that $\sigma_D = 2\,\mu L$ (determined experimentally at the flow rate of 25 μL/min, corresponding to $\langle v \rangle = 0.083$ cm/sec in a channel of $L = 10$ cm, $w = 0.01$ cm, and $b = 1$ cm) represents only 4 to 7% of the σ_V calculated from the Equation (19) for a monodisperse species, whose $D = 10^{-7}\,cm^2/sec$ retained in a hypothetical TFFF experiment carried out under these conditions. This σ_D value is largely below the imposed maximal value lying between 14 and 20%. When the σ_V was calculated for a smaller channel ($L = 10$ cm, $w = 0.005$ cm, $b = 0.5$ cm) and for the same linear velocity $\langle v \rangle = 0.083$ cm/sec, the $\sigma_D = 1\,\mu L$ decreased, due to slower flow rate (6.25 μL/min) and represents 14 to 25% of the σ_V, which is less favorable but still an acceptable value.

Although the contribution to the zone broadening, σ_D, should be almost zero for a detector integrated into the FFF channel, the practical advantage of the

external detectors is that the recently available devices represent much wider choices of the measured properties, giving a relevant response with respect to the detected matter. As a result, the tested detection system with the external measuring cell does not contribute significantly to the zone broadening of the retained species and is perfectly convenient for μ-TFFF.

The broadening caused by the injection system is less important due to the mentioned sharpening effect that is inherently related with the FFF retention mechanism. This was verified by using a large volume (5 μL) injection loop in some TFFF experiments. Regardless of the important increase of the injected volume (from 1 to 5 μL), the differences in the retention ratio R obtained for the PS standards were negligible. On the other hand, the increase of the zone width of the PS standards by about 30% when using the injection loop of 5 μL was not negligible. Consequently, the injection loop of 1 μL was utilized systematically in all TFFF experiments.

Polymer Fractionation

Polystyrene standards and THF were chosen because the molar masses of these samples are well determined and the THF is the most universal solvent for many polymers. The aim was to check the performance of the μ-TFFF of synthetic polymers in an ordinary range of molar masses, to demonstrate how the most important operational conditions can influence the fractionation, and to compare the μ-TFFF results with those obtained previously with the use of standard size TFFF channels.

The effect of the flow rate of the carrier liquid on the resolution was studied with a channel of the thickness $w = 0.01$ cm and the void volume $V_0 = 90$ μL. The temperature drop across the channel was kept at 35 K, with the temperature of the cold wall maintained at 293 K. The mixed solution (1 μL) of three PS of the molar masses 51,000, 115,000, and 411,000 g/mole was injected at various flow rates to demonstrate, qualitatively, the increase of the resolution with decreasing linear velocity of the carrier liquid from 0.166 to 0.0083 cm/sec. The fractograms in Figure 3 show clearly how the resolution of the individual PS progressively increases as the flow rate decreases. The resolution of three PS achieved at the lowest flow rate is comparable with that obtained previously (2) on a standard size TFFF channel, but in about half time. The influence of a decrease of the total concentration of the polymers in solution on the resolution is not evident from the fractograms in Figure 3 but, as will be described in the following paragraph, this effect should not, generally, be neglected. The heat flux 10× lower across this μ-TFFF channel in comparison with normal size TFFF channel (2), represents a net gain for the reasons mentioned in the Introduction.

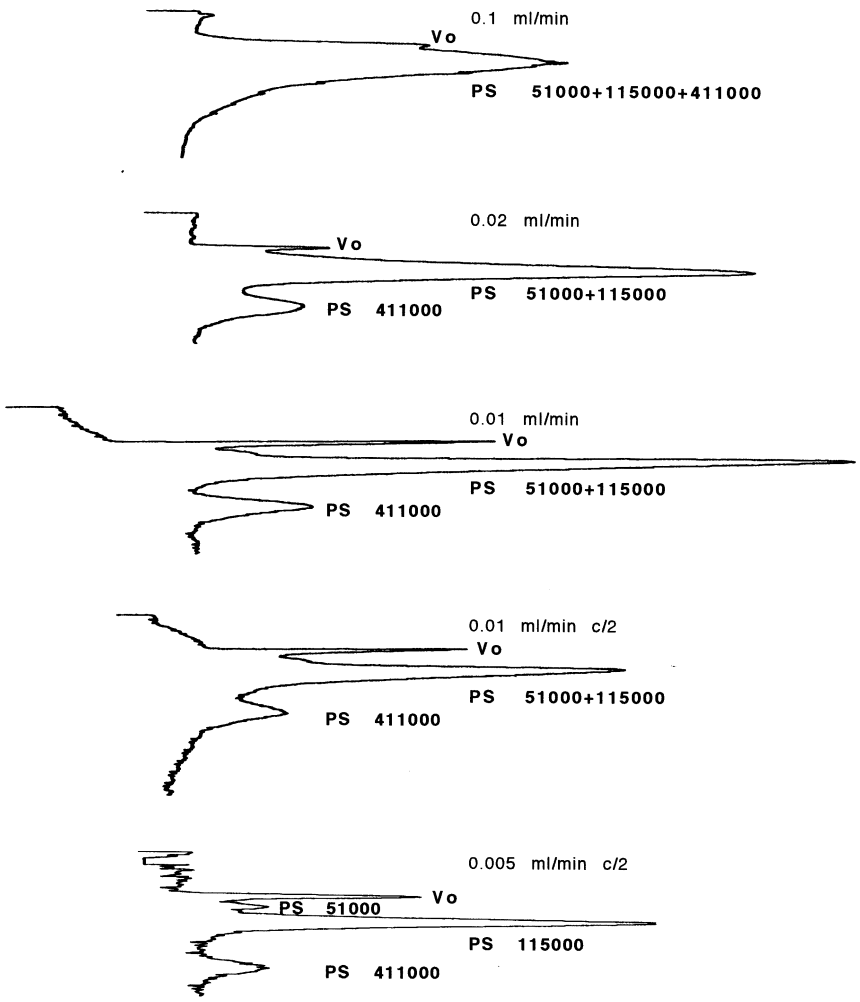

Figure 3. Resolution as a function of the flow rate in separation of three PS. Experimental conditions: channel dimensions $w = 0.01$ cm, $b = 1$ cm; linear velocities $\langle v \rangle = 0.166$, 0.033, 0.0166, and 0.0083 cm/sec; $\Delta T = 35$ K.

The effect of the concentration of the injected PS solutions was studied on various channels of different sizes w and b, and by applying various temperature drops across the channel. Some typical fractograms are shown in Figure 4. The most important differences, resulting from the variation of the concentration, are in the widths of the fractograms. The retention ratio does not vary very significantly.

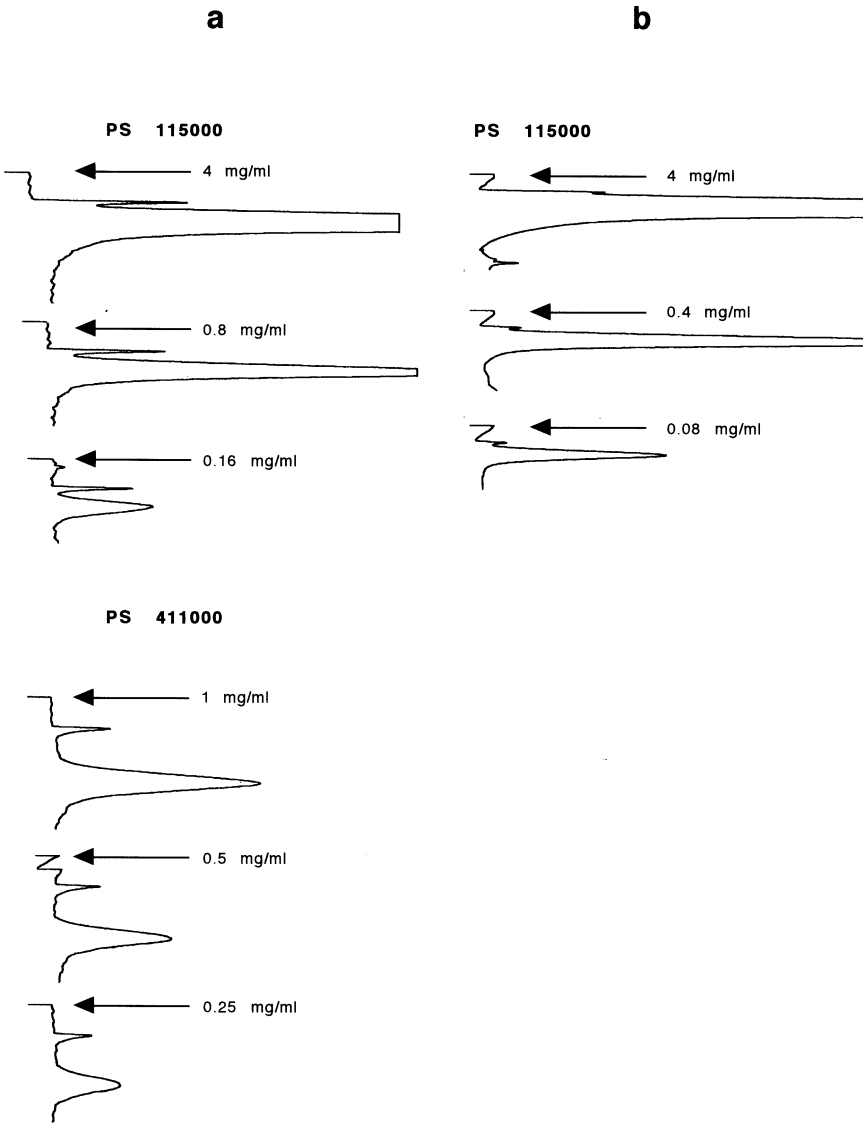

Figure 4. Effect of the concentration and injected volume of the PS samples of different molar masses. Experimental conditions: channel dimensions $w = 0.01$ cm, $b = 1$ cm; linear velocity $\langle v \rangle = 0.033$ cm/sec; a) injected volume 1 μL, $\Delta T = 35$ K, b) injected volume 5 μL, $\Delta T = 40$ K.

An important difference in the width of the resulting fractograms is due to the different injected volumes of the PS of molar mass 115 000 g/mole solutions (1 or 5 μL) shown in Figures 4a and 4b, respectively. Even with higher temperature drop applied, $\Delta T = 40$ K, whenever the injected volume was 5 μL, the resolution between the PS peak and the unretained marker peak is lower within the whole range of the tested concentrations (Figure 4b), compared with the injection of 1 μL at $\Delta T = 35$ K (Figure 4a). All experimental results concerning the effect of concentration are shown in Figures 5a and b, where the dependence of the retention ratio, R, and of the reduced peak width, w/V_0, on the specific viscosity of the injected PS solutions are plotted. The specific viscosity was chosen rather than the mass concentration, because the viscosity gradients (15) formed during the elution probably dominates (as in Size Exclusion Chromatography) the variation of the retention and/or of the width of the peak with the concentration, rather than the concentration dependent size of the macromolecules in solution. The curves in Figure 5a demonstrate that the retention ratio is slightly dependent on the specific viscosity within the whole range of the tested experimental conditions.

Unlike the retention ratio, the width of the fractograms is more strongly dependent on the specific viscosity of the injected PS solutions, and this dependence is more significant for a higher injected volume (5 μL) and also for a narrower channel ($b = 5$ mm). This observation seems to support the hypothesis that the viscosity gradients formed inside the channel play a major role in the observed dependencies of the retention ratio and of the peak width on the concentration. Although, the behavior of the flexible macromolecular chains at different concentrations in solution under conditions of TFFF is certainly more complex as already demonstrated by Caldwell et al., (16) from the practical analytical point of view, the μ-TFFF carried out at as low concentrations as possible can obtain accurate results. However, a detailed future study is necessary to determine more precisely the contributions of the particular phenomena to the observed concentration effects.

The effect of the temperature gradient was extensively studied for various polymer-solvent systems starting from the invention of TFFF (3,4) and new results are published (17). The intention of this work was to check whether the findings of previous studies can be confirmed on versatile μ-TFFF channels of various dimensions and, thus, to prepare a future investigation at extreme temperatures and temperature gradients which could not be achieved on standard size channels. The experimental results are summarized in Figure 6a as a plot of the retention ratio R vs. the molar mass M, obtained at different temperature drops, ΔT, across the channels of different dimensions (w and b). A simple conclusion, which follows from the results represented in Figure 6a, is that the obtained dependencies agree well with those found previously on classical TFFF channels, and with our theoretical predictions concerning the miniaturization of

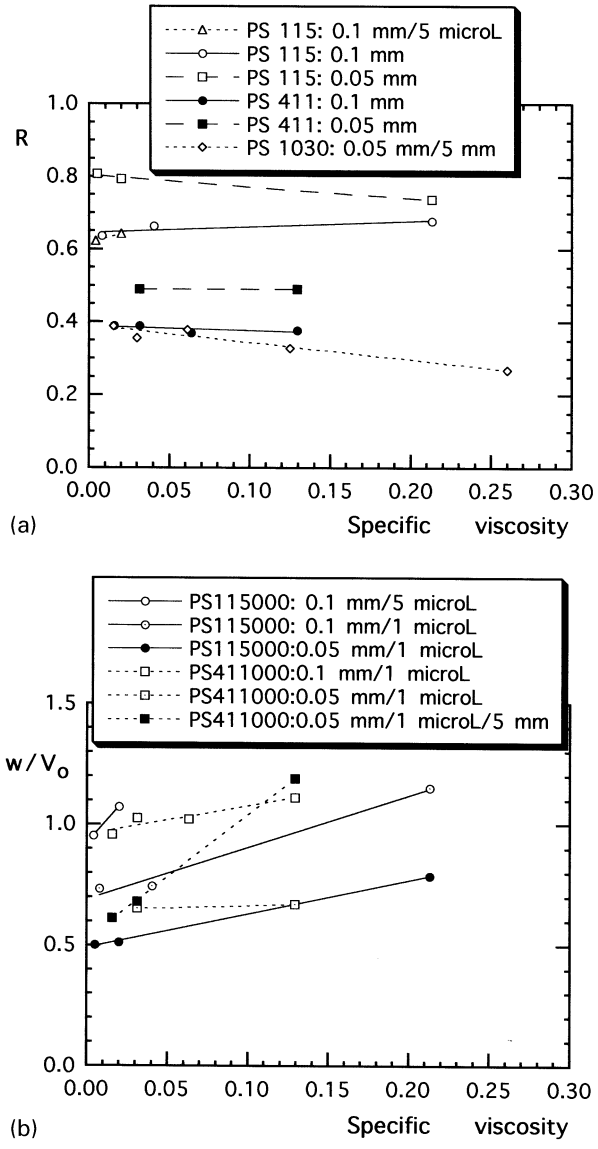

Figure 5. a) Dependence of the retention ratio R on the specific viscosity of injected solutions of the PS of different molar masses. Experimental conditions: channel dimensions $w = 0.01$ or 0.05 cm, $b = 1$ or 0.5 cm; linear velocity $\langle v \rangle = 0.033$ cm/sec; injected volume 1 or 5 μL; $\Delta T = 30$ K. b) Dependence of the normalized width w/V_0 of the fractograms on the specific viscosity of injected solutions of the PS of different molar masses. Experimental conditions: as in a).

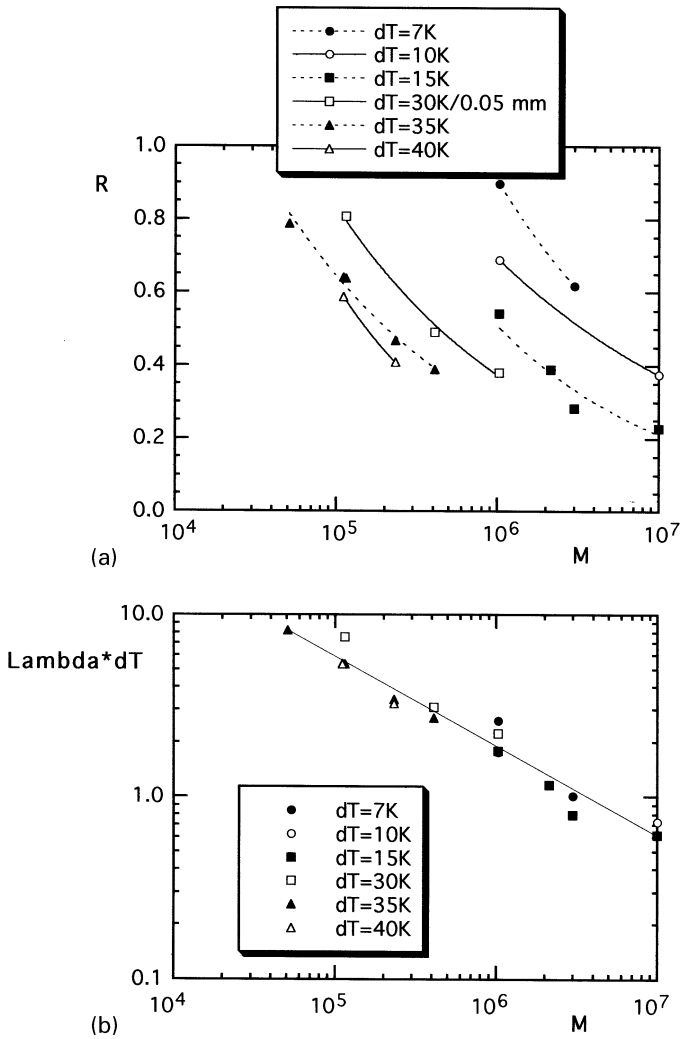

Figure 6. a) Dependence of the retention ratio R on the molar mass M of PS samples measured at various temperature drops ΔT across the channel. b) Dependence of the product $\Lambda\Delta T$ on the molar mass M of PS samples at various temperature drops ΔT across the channel.

the TFFF. The plot of $\lambda\Delta T$ vs. M, shown in Figure 6b, confirms the linearity of this dependence in log-log scale (found already by Gao et al. (18)) under the conditions of μ-TFFF and for the extended range of molar masses (including the molar mass over 10^6 g/mole). The relationship:

$$\log(\lambda\Delta T) = -0.50 \log M + 3.25 \tag{22}$$

found by the linear regression of the experimental points in Figure 6b is very close to that obtained by Gao et al. (18).

Fractionation of Ultra-High Molar Mass Polymers

Although, no physically significant definition of the ultra-high molar mass (UHMM) polymers exists, the molar masses over 1 or 2×10^6 g/mole are generally considered as ultra-high. The practical analytical reason for this choice is that the spectrum of the methods available to accurately determine the molar mass distribution (MMD) and various average molar masses is substantially reduced in this domain. In such a situation, the TFFF could represent a convenient alternative for the characterization of UHMM polymers.

Only few papers that appeared (18–22) on the TFFF of UHMM polymers exhibit some controversial interpretations of the experimental data:

a) Giddings et al. (19) explained the inverted elution order of the UHMM PS at a high flow rate ($\langle v \rangle = 2.68$ cm/sec) by the stress-induced diffusion of the macromolecular coils, which result in a formation of the focused zones eluting more rapidly compared with the normal (polarization) mode TFFF at low flow rates ($\langle v \rangle = 0.0715$ cm/sec). These authors (19) mention that a good deal of work was necessary to establish the appropriate conditions to demonstrate this focusing effect, but they do not give the details of their experiments.

b) Janca and Martin (20) published a detailed study of the TFFF of UHMM PS under various experimental conditions (concentration, flow rate, temperature gradient). The major conclusions were that the retention ratio and the whole shape of the fractograms of UHMM PS depend on the experimental conditions in agreement with the theoretical assumptions and experimental findings for "normal" polymers. The earlier elution of high molar mass samples at high flow rates was dependent on the initial relaxation period. A low diffusion coefficient of the polymers, in combination with a short elution time, does not allow establishing the trans-channel (mass transfer) steady state and, consequently, short or zero relaxation time (stop-flow time) resulted in lower elution volumes, because some part of the injected sample eluted with the highest linear

velocity at the central longitudinal axis of the channel. A frontal shoulder on the elution curve of the toluene in THF obtained when testing the injection-detection system of the present μ-TFFF channel, shown in Figure 7, is just a confirmation of Taylor's (23) famous experiments. Although, the diffusion coefficient of the toluene is at least $10^4 \times$ higher compared with that of the UHMM polymers, the mass transfer steady-state is not achieved on a given capillary during the elution time of 15 sec. As a result, the shear induced focusing effect cannot be explicitly confirmed on the basis of the realized TFFF experiments (19,20).

c) Chubarova and Nesterov (21) interpreted the TFFF fractograms obtained during a stay of EVCh in the laboratory of one author of this paper (JJ) as a proof of the shear degradation of UHMM PS under the conditions of the experiments. The principal objection against such an interpretation, is that the large unretained peaks appearing on the fractograms of the reinjected solutions of UHMM samples certainly correspond to the concentrated low molar mass impurities (products of THF oxidation), as has been proved experimentally (20). The attribution of these peaks to the products of shear degradation is

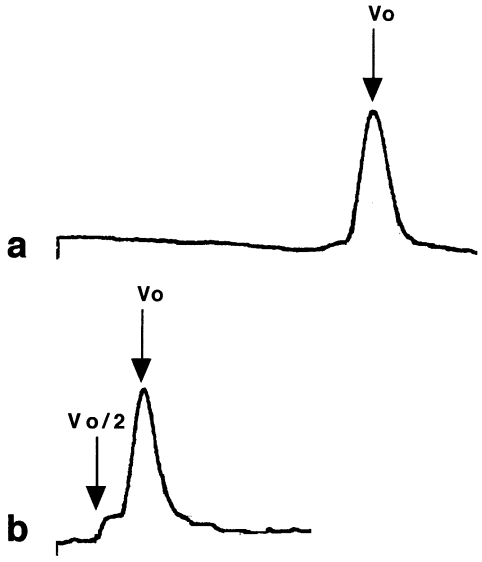

Figure 7. Elution curve of the toluene in THF on the μ-TFFF channel (a) and on a short capillary (b) connecting directly the injection and detection system without the channel.

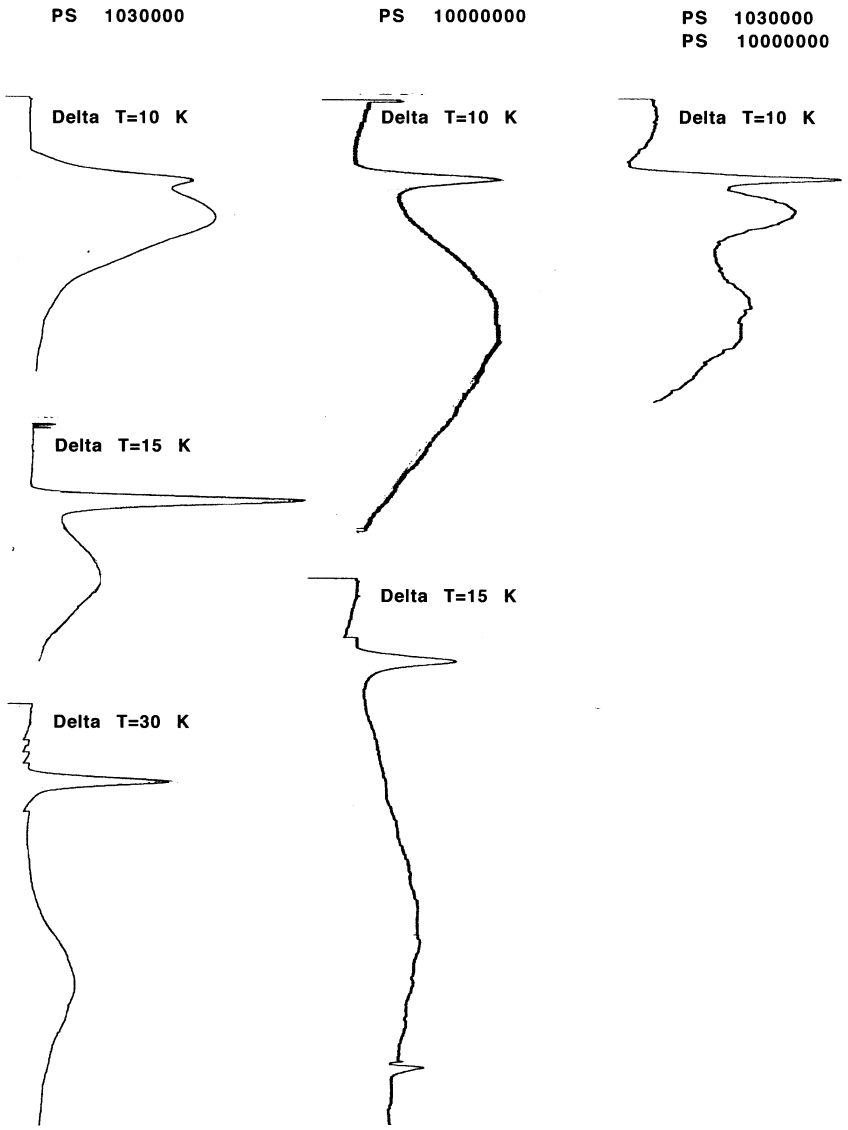

Figure 8. Retention and separation of two ultra-high molar mass PS at different temperature drops ΔT. Experimental conditions: channel dimensions $w = 0.01$ cm, $b = 1$ cm; linear velocity $\langle v \rangle = 0.033$ cm/sec.

pure speculation not justified by any experimental proof. Another unjustified speculation (21) is that lower retention ratio of the UHMM PS at high flow rates is due to the focusing effect. The relaxation phenomena, which might explain the inverted elution order of the UHMM polymers, were not considered at all (21).

The experimental results obtained in this work with the μ-TFFF channel are included in Figures 5 and 6 and some of the most interesting fractograms are represented in Figure 8. The retention order of the UHMM PS obtained at low flow rates confirmed the normal polarization mechanism of the separation and very good reproducibility of the experiments, as concerns the retention and shape of the fractograms, regardless of relatively high polydispersity of some PS samples. The reproducible oscillations on the fractograms described previously (21) and considered to be Rayleigh-Taylor hydrodynamic instabilities, were not observed under the conditions of the μ-TFFF.

Figure 8 shows the fractograms of two UHMM PS obtained at various temperature gradients separately and in a mixture. A good resolution between two peaks of the PS mixture demonstrates high performance of the μ-TFFF regardless of relatively broad MMD of both PS samples. As a result, if the μ-TFFF of UHMM polymers is accurately carried out, there is no principal reason to obtain irregular and/or irreproducible fractograms.

CONCLUSIONS

The theoretical analysis has demonstrated the ways of keeping or increasing the performance of Thermal FFF by reducing, substantially, the size of the separation channel. It has been shown that the increase of the temperature drop across the channel has a more significant impact on the efficiency, compared with a decrease of the channel thickness. However, the physical properties of the carrier liquid, especially the boiling point, can limit the applicability of this principle even when using the pressurized TFFF system permitting work above the critical temperature at the atmospheric pressure.

The miniaturization of the channel permits work within a more extensive range of the temperatures and temperature gradients, because the tap water frequently used for the cooling can be more easily replaced by the thermostated circulating liquid, without a need to use high power refrigerating systems. This is due to a substantial decrease of the heat flux across the μ-TFFF channels.

The miniaturization, together with a rationalized design, leads to a simplified manipulation and an increased versatility of the channel. An important theoretical and experimental finding is that the currently available injection and

detection systems can be used without increasing the extra-channel zone broadening over the limits of the acceptable experimental errors.

The practical model applications of the μ-TFFF channel for the separations of macromolecules up to UHMM polymers, confirmed that the efficiency is comparable or higher than that obtained with classical size channels, in agreement with the theoretical predictions.

The μ-TFFF channel opens the possibility of coupling this high performance separation technique with highly selective detection systems, such as mass spectroscopy, thus enlarging the potentials of the analysis and characterization of polymers and colloidal particles. The economical factors resulting from an important decrease of the energy and carrier liquid consumption should not be neglected, in addition to a reduced sample amount needed for one analysis, which can be as small as a few nanograms.

ACKNOWLEDGMENTS

Financial support of Conseil Regional Poitou-Charentes and technical assistance of Mrs. T. V. Shishkanova in experimental work are gratefully acknowledged.

REFERENCES

1. Thompson, G.H.; Myers, M.N.; Giddings, J.C. Sepn. Sci. **1967**, *2*, 797.
2. Giddings, J.C.; Myers, M.N.; Janca, J. J. Chromatogr. **1978**, *186*, 37.
3. Janca, J. *Field-Flow Fractionation: Analysis of Macromolecules and Particles*; Marcel Dekker, Inc.: New York, 1988.
4. Schimpf, M.E.; Caldwell, K.D.; Giddings, J.C. *Field-Flow Fractionation Handbook*; John Wiley & Sons: New York, 2000.
5. Shiundu, P.M.; Giddings, J.C. J. Chromatogr. A, **1995**, *715*, 117.
6. Mes, E.P.C.; Tijssen, R.; Kok, W.Th. J. Chromatogr. A, **2001**, *907*, 201.
7. Giddings, J.C. J. Microcolumn Sep. **1993**, *5*, 497.
8. Giddings, J.C.; Martin, M.; Myers, M.N. J. Chromatogr. **1978**, *158*, 419.
9. Hovingh, M.E.; Thompson, G.H.; Giddings, J.C. Anal. Chem. **1970**, *42*, 195.
10. Giddings, J.C.; Yoon, J.H.; Caldwell, K.D.; Myers, M.N.; Hovingh, M.E. Separ. Sci. **1975**, *10*, 447.
11. Brandrup, J.; Immergut, E.H. *Polymer Handbook,* 3rd Ed.; John Wiley & Sons: New York, 1989.
12. Martin, M.; Jaulmes, A. Separ. Sci. Technol. **1981**, *16*, 691.
13. Janca, J. J. Liq. Chromatogr. **1981**, *4*, 181.

14. Gale, B.K.; Caldwell, K.D.; Frazier, A.B. Abstract L17, 8th Int. Symp, on FFF, Paris, 1999.
15. Janca, J. Anal. Chem. **1979**, *51*, 637.
16. Caldwell, K.D.; Brimhall, S.L.; Gao, Y.; Giddings, J.C. J. Appl. Polym. Sci. **1988**, *36*, 703.
17. Schure, M.R. http://www.rohmhaas.com/fff.
18. Gao, Y.S.; Caldwell, K.D.; Myers, MN.; Giddings, J.C. Macromolecules **1985**, *18*, 1272.
19. Giddings, J.C.; Li, S.; Williams, P.S.; Schimpf, M.E. Makromol. Chem. Rapid Commun. **1988**, *9*, 817.
20. Janca, J.; Martin, M. Chromatografia **1992**, *34*, 125.
21. Chubarova, E.V.; Nesterov, V.V. In: *Strategies in Size Exclusion Chromatography*; Potschka, M., Dubin, P.L., Eds.; ACS Symposium Ser.; Am. Chem. Soc.: Washington, D.C., 1996; Vol. 635, 127.
22. Lee, S.; Kwon, O.S. In *Chromatographic Characterization of Polymers, Hyphenated and Multidimensional Techniques*; Provder, T., Barth, H.G., Urban, M.W., Eds.; ACS Symposium Ser.; Am. Chem. Soc.: Washington, D.C., 1995; Vol. 247, 93.
23. Taylor, G. Proc. Roy. Soc. A **1953**, *219*, 186.

Received September 30, 2001
Accepted October 17, 2001
Manuscript 5661